Methylene Blue Inhibits Amyloid Aβ Oligomerization by Promoting Fibrillization†

Mihaela Necula,‡ Leonid Breydo,‡ Saskia Milton,‡ Rakez Kayed,‡ Wytze E. van der Veer,§ Paul Tone,|| and Charles G. Glabe*,‡

Department of Molecular Biology and Biochemistry, University of California, Irvine, California 92697, Department of Chemistry, University of California, Irvine, California 92697, Department of Medicine, St. Vincent Catholic Medical Centers, Staten Island Division, Staten Island, New York 10310, and New York Medical College, Valhalla, New York 10595

Received February 28, 2007; Revised Manuscript Received May 16, 2007

ABSTRACT: Amyloid plaques are hallmark neuropathological lesions in Alzheimer's disease, which consist of abnormally aggregated Aβ protein. Multiple Aβ aggregated species have been identified, and neurotoxicity appears to be correlated with the amount of nonfibrillar oligomers. Therefore, selective inhibition of Aβ oligomer formation has emerged as an attractive means of therapeutic intervention. To investigate whether small molecules can modulate aggregation to achieve selective inhibition of neurotoxic amyloid oligomers, Aβ aggregation was assayed in vitro in the presence of methylene blue, using immunoreactivity with the prefibrillar oligomer-specific antibody A11, transmission electron microscopy, and turbidity assays. Methylene blue inhibited oligomerization when used at substoichiometric concentrations relative to that of the Aβ monomer. Inhibition of Aβ oligomerization was achieved concomitant with promotion of fibrillization, suggesting that oligomer and fibril formation are distinct and competing pathways. Methylene blue-mediated promotion of fiber formation occurred via a dose-dependent decrease in the lag time and an increase in the fibrillization rate, consistent with promotion of both filament nucleation and elongation. Addition of methylene blue to preformed oligomers resulted in oligomer loss and promotion of fibrillization. The data show that Aβ oligomer formation is inhibited by promoting fibril formation, which suggests that the relative pathological significance of oligomers and fibrils may be tested in vivo using methylene blue. If Aβ oligomers represent the primary pathogenic species, then inhibition of this highly toxic species via promotion of formation of less toxic aggregates may be therapeutically useful.

Alzheimer's disease (AD)[1] is a neurodegenerative disease characterized, in part, by the accumulation of amyloid β protein (Aβ) into fibrillar plaques in select areas of the brain (*2*). Aβ fibrillization has been described as a nucleation-dependent process (*3*, *4*) that has as an end point the formation of fibers characterized by classical amyloid morphology and tinctorial properties. Early studies suggested that Aβ fibers are toxic (*5*−*9*), and therefore, tremendous effort was oriented toward screening small molecules for the ability to arrest fibrillization and resulted in the identification of numerous inhibitors (*9*−*24*). The therapeutic premise extended further to the screening for small molecules that inhibit Aβ-mediated toxicity (*9*, *14*, *16*, *17*, *25*). However, more recent evidence indicates that soluble Aβ oligomers may represent the primary pathological species rather than fibrils. There is a poor correlation between the extent of Aβ fibrillar deposition and the severity of AD (*26*), and oligomers are more toxic in vitro and in vivo than fibrils (*27*−*34*). In addition, soluble Aβ oligomers appear to correlate better with the severity and localization of neurodegeneration (*35*, *36*). This poses the question of whether some inhibitors of fibrillization might exacerbate pathology by promoting oligomer formation.

Mechanisms underlying oligomerization and fibril formation also require clarification. Aβ assembly appears to be more complicated than a simple transition from a soluble monomer to fibrils. A growing body of evidence suggests that aggregation occurs via multiple pathways (*37*, *38*) that are populated by morphologically and immunologically distinct Aβ aggregated species, including oligomers, protofibrils, and annular protofibrils (*1*, *27*, *39*−*45*). However, whether oligomers are "on pathway" intermediates for fiber formation that condense en bloc into fibrils (*40*, *46*−*51*) or represent "off pathway" species that serve to buffer monomer concentration is still under debate (*52*−*54*). Taken together, these observations indicate a need for clarifying the relationships between Aβ oligomers and fibrils and refocus thera-

† This work was supported by grants from the National Institutes of Health (NIH NS 31230) and from the HighQ and Larry L. Hillblom foundations.

* To whom correspondence should be addressed: Department of Molecular Biology and Biochemistry, University of California, 3438 McGaugh Hall, Irvine, CA 92697. Telephone: (949) 824-6081. Fax: (949) 824-8551. E-mail: cglabe@uci.edu.

‡ Department of Molecular Biology and Biochemistry, University of California.

§ Department of Chemistry, University of California.

|| St. Vincent Catholic Medical Centers and New York Medical College.

[1] Abbreviations: AD, Alzheimer's disease; Aβ, amyloid β peptide; Aβ_{40}, amyloid β peptide containing 40 amino acids; Aβ_{42}, amyloid β peptide containing 42 amino acids; AR, horseradish peroxidase-conjugated anti-rabbit IgG; BSA, bovine serum albumin; CNS, central nervous system; HCl, hydrochloric acid; HFIP, 1,1,1,3,3,3-hexafluoroisopropanol; MB, methylene blue; PBS, phosphate-buffered saline; SDS, sodium dodecyl sulfate; TBS-T, Tris-buffered saline containing 0.01% Tween 20; TEM, transmission electron microscopy; ThT, thioflavin T; TMB, 3,3′,5,5′-tetramethylbenzidine.

10.1021/bi700411k CCC: $37.00
Published on Web 06/27/2007

peutic intervention toward targeting oligomers and protofibrils (*24*, *55*−*59*).

Methylene blue (MB) belongs to the phenothiazine class of compounds and has many properties required for drug candidates expected to act in the central nervous system (CNS). Of these, its high solubility in aqueous media, its low toxicity in rats and humans (*60*, *61*), its ability to cross the blood−brain barrier (*62*), and its approval for use in humans (*61*, *63*) are especially attractive as a potential therapeutic. MB is able to act at CNS sites, as indicated by its use in the treatment of ifosfamide encephalopathy (*61*) and prevention of bacterial lipopolysaccharide-induced fever in rabbits. The later occurs by blocking the production of reactive oxygen species, a reaction mediated through the CNS (*64*). Besides having general characteristics that make it suitable for targeting diseases of the CNS, MB appears to restore spatial memory retention in rats with impaired mitochondrial respiration (*60*, *65*). However, this beneficial activity likely results from a MB-induced increase in the level of oxygen consumption (*60*) and has not been linked to protein aggregation.

MB has been reported to inhibit both recombinant tau and Aβ_{40} fibrillization in vitro (*66*), with IC_{50} values in the low micromolar range. Phenothiazines related to MB have also been shown to inhibit the conversion of soluble prion protein into the protease-resistant form (*67*−*70*). In addition, MB has been reported to destabilize tau paired helical filaments when used at high concentrations (*71*). However, when MB was added to recombinant filamentous tau, it supported a further increase in the amount of aggregated tau (*66*). Because of the conflicting reports about the activity of MB on amyloid aggregation and its potential as a human therapeutic, we sought to clarify the mechanism of action of MB with respect to its activity on oligomer and fibril formation. Here we report that MB has two distinct effects on Aβ_{42} assembly. It inhibits oligomerization and enhances fibril formation, suggesting that Aβ_{42} oligomerization and fibrillization pathways are distinct and that MB stabilizes an amyloidogenic conformation that favors fibrillization.

EXPERIMENTAL PROCEDURES

Materials. Synthetic Aβ_{42} was prepared as previously described (*72*). Formvar/carbon-coated nickel grids (200 mesh) were obtained from Electron Microscopy Sciences (Ft. Washington, PA). Ninety-six-well clear, flat bottom microplates were obtained from Nalge Nunc International (Rochester, NY), and 3,3′,5,5′-tetramethylbenzidine was from KPL (Gaitherburg, MD). Horseradish peroxidase-conjugated anti-rabbit IgG (AR) was purchased from Promega (Madison, WI); 6E10 and 4G8 antibodies were from Signet (Dedham, MA), and the ECL chemiluminescence kit was from Amersham-Pharmacia (Piscataway, NJ). Nitrocellulose membranes (0.2 μm) were form Schleicher & Schuell. The 4 to 20% Tris-HCl gels were from Bio-Rad (Hercules, CA). Stock solutions of MB dissolved in water were from Bioniche TEO. All other reagents were from Sigma (St. Louis, MO).

Aβ_{42} Oligomerization and Fibrillization. Aβ_{42} stock solutions (2 mM) were obtained by dissolving the lyophilized peptide in 100 mM NaOH followed by water bath sonication for 30 s. The oligomerization reaction was initiated by diluting the stock solution in phosphate-buffered saline (PBS, pH 7.4) and 0.02% sodium azide (final Aβ_{42} concentration of 45 μM). The reaction tubes were covered with aluminum foil to exclude light and maintained on a benchtop at room temperature for up to 10 days in the absence or presence of MB (final concentrations of 0.01−445 μM). We refer to these conditions as "oligomerization conditions". Since MB is known to be a photoreactive initiator of free radical oxidative reactions, we included sodium azide as a singlet oxygen scavenger and for prevention of microbial growth. Mass spectroscopic analysis of Aβ incubated under these conditions in the presence of MB indicates that approximately 20% of the peptide is singly oxidized (presumably at methionine 35), while approximately 10% is oxidized in the absence of MB. The oligomerization reactions were assayed by dot blot, ELISA, Western blot, and transmission electron microscopy (TEM), as described below. For fibrillization, Aβ_{42} stock solutions (2 mM) were obtained by dissolving the lyophilized peptide in 100 mM NaOH followed by water bath sonication for 30 s. Fibrillization (final Aβ_{42} concentration of 45 μM) was initiated by diluting the stock solution in 10 mM HEPES, 100 mM NaCl, and 0.02% sodium azide (pH 7.4). We refer to these conditions as "fibrillization conditions". The reaction mixtures were stirred at room temperature for up to 8 days, in the presence and absence of MB (final concentrations of 0, 10, 30, 100, 300, and 445 μM). The reactions were assayed by turbidity and TEM, as described below. To determine the effect of MB on preformed oligomers, Aβ_{42} oligomers were prepared by incubation for 4 days under the oligomerization conditions described above and divided into several aliquots. One aliquot served as the control, and the remaining aliquots were treated with MB (final concentrations of 0.01−445 μM). The reactions were assayed by ELISA and TEM as described below, 2 and 7 days after MB addition, respectively. MB was supplied from serially diluted stocks in H_2O, and the carryover volume was $\leq$1.67%.

Dot Blot Assay. The dot blot assay was performed as previously described (*1*) to detect Aβ_{42} oligomer formation. Briefly, 2 μL aliquots of each reaction were applied onto nitrocellulose membranes. The membranes were blocked (1 h at room temperature or overnight at 4 °C) with 10% nonfat milk dissolved in Tris-buffered saline containing 0.01% Tween 20 (TBS-T). Sodium azide (0.02%) was added for overnight blocking. The membranes were then washed and incubated with affinity-purified anti-oligomer antibody (A11)[2] (*1*) (1:1500 dilution in TBS-T containing 5% milk) for 1 h at room temperature. The membranes were washed again and incubated with horseradish peroxidase-conjugated anti-rabbit IgG (AR) diluted 1:5000 in TBS-T containing 5% milk for 1 h at room temperature. The blots were then washed and developed with the ECL chemiluminescence kit. Separate membranes serving as controls for the presence of Aβ_{42} were treated as described above, except that the A11 and AR antibodies were replaced with 6E10 or 4G8 and horseradish peroxidase-conjugated anti-mouse IgG, respectively. These antibodies were diluted 1:10000 in TBS-T containing 3% BSA. All washes were performed with TBS-T three times

[2] Nomenclature: A11, anti-oligomer-specific antibody (*1*). Inhibition of oligomerization refers to inhibition of formation of A11-immunoreactive oligomers. Oligomerization conditions refer to conditions that favor A11-reactive oligomer formation that is fiber-free at early time points. Fibrillization conditions refer to conditions that favor fiber formation in the absence of A11-reactive oligomers.

for 5 min each except for the last wash before detection, which was for 10 min.

ELISA. An ELISA was performed as previously described (*1*). Briefly, Aβ_{42} was subjected to oligomerization in the absence and presence of MB (0.01−445 μM), as described above. In addition, MB was added to preformed Aβ_{42} oligomers in the same concentration range. Aliquots of each aggregation and disaggregation reaction were applied to 96-well clear, flat bottom microplates containing 100 μL of coating buffer [0.1 M sodium bicarbonate (pH 9.6)]. The Aβ_{42} concentration used was within the linear range of the assay. The plates were incubated for 2 h at 37 °C, washed, blocked with 10% BSA and TBS-T for 2 h at 37 °C, and washed again. Then, 100 μL of A11 antibody (1:1500 dilution in a 3% BSA/TBS-T mixture) was added to each well, and the plates were incubated for 1 h at 37 °C. After the samples had been washed, 100 μL of AR antibody (1:5000 dilution in a 3% BSA/TBS-T mixture) was added to each well, and the plates were incubated for 1 h at 37 °C. The plates were then washed and developed with 3,3′,5,5′-tetramethylbenzidine (TMB). The reactions were stopped with 100 μL of 1 M HCl and assayed by absorbance at 450 nm. PBS was used for all washes which were performed three times. Each reaction was performed in triplicate, and the data points were fit, as described previously (*73*), to the dose−response curve:

$$y = y_{\min} + \frac{y_{\max} - y_{\min}}{1 + 10^{(\log x - \log \mathrm{IC}_{50})n}} \quad (1)$$

where y_{max} is the amount of oligomer measured in the absence of MB, defined as 100% oligomerization, y is the amount of oligomer measured in the presence of MB used at concentration x, y_{min} is the amount of oligomer remaining in the presence of MB, n is the Hill coefficient, and IC_{50} is defined as the concentration of MB required to attain half-maximal inhibition of oligomerization. y and y_{min} were expressed as the percent absorbance in the absence of MB. The fit was obtained using Sigmaplot (Systat Software Inc., Point Richmond, CA). All data were corrected by subtraction of the signal corresponding to control reactions containing MB only.

Western Blot. Aliquots (10 μL) of each Aβ_{42} oligomerization reaction, treated with MB or controls, were mixed in a 1:1 ratio (v/v) with 2× SDS sample buffer, boiled for 5 min, and loaded onto 4 to 20% Tris-HCl gels. Aliquots of Aβ_{42} fibers formed under fibrillization conditions were subjected to the same treatment. The gels were transferred to nitrocellulose membranes which were then subjected to the dot blot assay with A11 and 6E10 antibodies, as described above.

Electron Microscopy. Aliquots (1 μL) of Aβ_{42} oligomerization, fibrillization, and oligomer disaggregation reactions were adsorbed onto 200 mesh Formvar/carbon-coated nickel grids until they were dry. The grids were then washed with water, stained with 2% uranyl acetate, and washed again. The grids were allowed to dry between all steps and were viewed with a Phillips CM 12 microscope operated at 65 kV.

Turbidity Measurements. Aβ_{42} was incubated under fibrillization conditions in the presence and absence of MB for 8 days. Each reaction was then assayed by turbidity at a wavelength of 400 nm, to estimate the amount of fibrillar material. Aliquots of reaction mixtures containing MB in the absence of Aβ_{42} were used to blank the spectrophotometer. These blanks are appropriate because MB does not change its adsorption properties in the presence of nonaggregated, oligomeric, and fibrillar Aβ_{42} (data not shown). Each data point is an average of triplicate readings.

Each curve (0−100 μM MB) was fit to the sigmoidal equation (*74*−*77*):

$$y = y_0 + \frac{A}{\left(1 + \mathrm{e}^{-\dfrac{t - t_{50}}{\tau}}\right)} \quad (2)$$

where y is the turbidity or filament mass at time t, y_0 is the filament mass at time zero, A represents the maximum filament mass at equilibrium (maximum turbidity), t_{50} corresponds to the time to attain half-maximal fibrillization, and $1/\tau$ is the apparent first-order rate constant for fibril growth. The lag times, defined as the time where the tangent to the point of maximum fibrillization rate intersects the abscissa (*78*), were calculated as $t_{50} - 2\tau$ (*74*−*77*) and were assumed to reflect filament nucleation (*79*). The fibrillization rate at t_{50}, k_{50}, was calculated as $1/t_{50}$.

In the presence of 300 and 445 μM MB, each curve represents a fit of the data points to the rectangular hyperbola (*76*)

$$y = \frac{at}{t_{50} + t} \quad (3)$$

where y is the turbidity or filament mass at time t, a represents the maximum turbidity (maximum filament mass), and t_{50} corresponds to the time to half-maximal turbidity. The fibrillization rate at t_{50} (50% fibrillization rate), k_{50}, was calculated as $1/t_{50}$.

The k_{50} calculated in the absence of MB as described above was subtracted form all other rates, and the resultant corrected 50% fibrillization rates, $k_{50}^{\mathrm{corrected}}$, were expressed as a function of MB concentration and fit to the rectangular hyperbola

$$k_{50}^{\mathrm{corrected}} = \frac{k_{50}^{\max} x}{x_0 + x} \quad (4)$$

where $k_{50}^{\mathrm{corrected}}$ is the corrected 50% fibrillization rate corresponding to MB concentration x, $k_{50}^{\max}$ represents the corrected maximum 50% fibrillization rate, and x_0 is the MB concentration required to attain a half-maximal corrected 50% fibrillization rate. All fits were obtained using Sigmaplot.

RESULTS

Methylene Blue Inhibits Aβ_{42} Oligomerization. We investigated whether MB inhibits Aβ_{42} oligomer formation using the oligomer-specific antibody A11 to detect oligomers on dot blots (*1*). Untreated control reaction mixtures and reaction mixtures treated with MB (final concentrations of 1, 30, and 445 μM) were incubated at room temperature, without stirring for up to 10 days under oligomerization conditions described in Experimental Procedures. We previously showed that under these conditions Aβ_{42} forms a morphologically

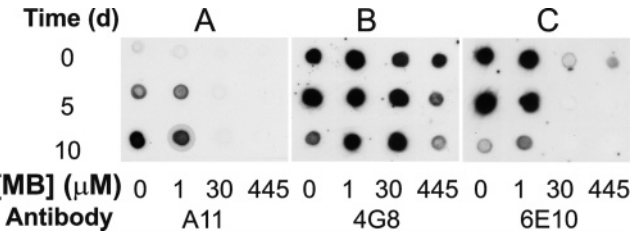

FIGURE 1: Methylene blue inhibits Aβ_{42} oligomerization. Aβ_{42} (45 μM, final concentration from freshly dissolved stock solutions) was incubated for up to 10 days in PBS (pH 7.4) at room temperature without stirring (oligomerization conditions), in the absence or presence of MB (10, 30, and 445 μM). Aliquots were removed at various time points during aggregation, spotted onto nitrocellulose membranes, and probed with A11 (A), 4G8 (B), and 6E10 antibodies (C). (A) The control reaction (0 μM MB) developed time-dependent oligomer-specific immunoreactivity that became strong after incubation for 5 days and was stable for extended periods of time, indicative of oligomer formation. MB inhibited the oligomer immunoreactivity in a dose-dependent manner. The intensity of each dot reflects the amount of oligomer present in each reaction mixture, probed with the oligomer-specific antibody A11. (B) Most samples developed strong 4G8 immunoreactivity, indicative of the presence of Aβ_{42} on the membranes. Decreased 4G8 immunoreactivity observed at 445 μM MB is attributed to the loss of epitopes and weakened Aβ_{42} binding to the membranes caused by fibrillization and clumping. (C) Control reaction mixtures and mixtures containing small amounts of MB developed strong 6E10 immunoreactivity. Decreased 6E10 immunoreactivity at later time points in these reactions and in reaction mixtures containing high MB concentrations is attributed to the loss of 6E10 epitopes, Aβ_{42} aggregation, and weakened binding of Aβ_{42} to membranes.

heterogeneous population of A11-immunoreactive oligomers that, at early time points (<6 days), are fiber-free (*37*). Five days after initiation of oligomerization, the control reaction developed A11 immunoreactivity that increased gradually in intensity, indicative of oligomer formation (Figure 1A). MB partly inhibited Aβ_{42} oligomer formation when used at low concentrations (1 μM). However, concentrations of MB of $\geq$30 μM completely inhibited oligomer-specific antibody immunoreactivity, indicative of strong inhibition of Aβ_{42} oligomerization (Figure 1A). Control membranes probed with 4G8 and 6E10 antibodies showed diminishing immunoreactivity upon prolonged incubation of Aβ_{42} under oligomerization conditions in the absence of MB (Figure 1B,C). This phenomenon has been described previously and has been attributed to the loss of 4G8 and 6E10 epitopes concomitant with the appearance of A11 binding sites (*37*). In the presence of low MB concentrations (1 and 30 μM), 4G8 immunoreactivity remained strong for the entire experimental period, showing that MB did not interfere with the binding of Aβ_{42} to the nitrocellulose membrane (Figure 1B). Therefore, the loss of A11 immunoreactivity observed in the presence of MB was a result of MB-mediated oligomer loss. 6E10 immunoreactivity is significantly more sensitive to MB than 4G8 immunoreactivity (Figure 1B,C), indicating that MB has profound effects on the exposure of this amino-terminal epitope.

Effect of Methylene Blue on Aβ_{42} Oligomerization. To confirm the inhibitory activity of MB on oligomerization, Aβ_{42} was incubated under oligomerization conditions for 5 days in the absence (control reaction) and presence of MB (300 μM), as described in Experimental Procedures. Aliquots of each reaction were assayed by Western blotting with A11 and 6E10 antibodies along with aliquots of fibrillar Aβ_{42}

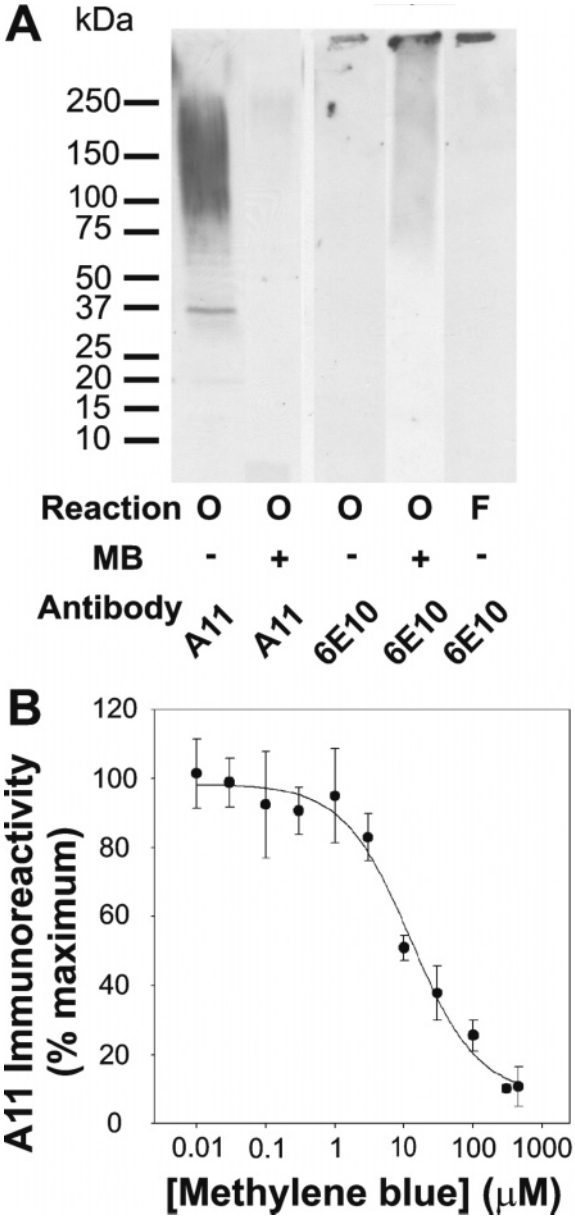

FIGURE 2: Effect of MB on oligomerization. (A) Aβ_{42} was incubated under oligomerization conditions (O) without stirring (45 μM, final concentration) for 5 days in the absence (control reaction) or presence of MB (300 μM). Each reaction was assessed for immunoreactivity with anti-oligomer-specific antibody A11 and 6E10 by Western blotting. MB abolished A11 immunoreactivity, consistent with inhibition of Aβ_{42} oligomerization, and promoted the formation of higher-order aggregates that were stained by 6E10 at the top of the gel. Fibrils (F) prepared under fibrillization conditions in the absence of MB also accumulated at the top of the gel and stained with 6E10. (B) Aβ_{42} was incubated under oligomerization conditions without stirring (45 μM, final concentration) for 5 days in the absence (control reaction) or presence of MB (0.01−445 μM). Oligomer formation was assayed by an ELISA using anti-oligomer-specific antibody A11. Each data point was obtained in triplicate and was expressed as the percent absorbance of the control reaction $\pm$ the standard deviation. The curve represents the best fit of the data points to eq 1 and was used to determine the IC_{50}.

prepared under fibrillization conditions in the absence of MB. A high concentration of MB was used to effect complete inhibition of oligomerization, based on the results obtained with the dot blot assay. Control Aβ_{42} oligomers were reactive with the A11 antibody in the molecular mass range of ~36−250 kDa (Figure 2A). Although most of the A11 immunore-

activity appears as a broad band between 75 and 250 kDa, a discrete 36 kDa band was also observed. Oligomers with molecular masses of <250 kDa obtained under these conditions do not react with 6E10 antibody (Figure 2A), consistent with the results obtained by dot blots (Figure 1C). A weak 6E10-immunoreactive band was observed at the top of the gel in control reactions, indicative of the appearance of small amounts of fibrillar material, which was expected upon prolonged incubation of Aβ_{42} under oligomerization conditions (*37*). MB-treated samples did not exhibit A11 immunoreactivity (Figure 2A), confirming that this compound inhibits Aβ_{42} oligomerization. However, MB treatment significantly increased the amount of 6E10-immunoreactive Aβ_{42} that accumulates at the top of the gel and is not stained by A11. The band localized at the top of the gel is also prominent in fibrillar Aβ_{42} samples, suggesting that MB drives the accumulation of increased amounts of high-molecular mass Aβ_{42} fibrils compared to control reactions.

To determine the inhibitory potency of MB, Aβ_{42} was subjected to oligomerization under conditions described in Experimental Procedures, in the absence (control reaction) or presence of MB at concentrations ranging from 0.01 to 445 μM. After incubation for 5 days, aliquots of each reaction were assayed by an ELISA with the anti-oligomer antibody A11. The IC_{50} for inhibition of Aβ_{42} oligomerization determined from the dose−response curve (eq 1) was 12.48 ± 3.28 μM (Figure 2B). Taken together, these data confirm that MB inhibits Aβ_{42} oligomerization at substoichiometric concentrations relative to Aβ_{42} monomer and suggest that MB may bind to small oligomers.

Mechanism of Methylene Blue-Mediated Inhibition of Aβ_{42} Oligomerization. The accumulation of high-molecular mass aggregates at the top of gels when Aβ_{42} is treated with MB under oligomerization conditions is similar to that observed in reaction mixtures that contain Aβ_{42} fibers formed in the absence of MB under fibrillization conditions (Figure 2A). These data suggest that the loss of A11 immunoreactivity observed in the presence of high concentrations of MB on dot blots, western blots, and ELISA assays may be the result of aggregation of Aβ_{42} into fibrils. To confirm these observations and assess the nature of the aggregated material, Aβ_{42} was incubated under oligomerization conditions for 5 days in the absence (control reaction) and presence of MB. Aliquots of each aggregation reaction were imaged by TEM at various time points. Consistent with previous observations (*37*), Aβ_{42} exhibited minimal aggregation at time zero in the control reaction (Figure 3A) and assembled into a heterogeneous population of oligomers and protofibrils, after incubation for 5 days (Figure 3C,E). In the presence of 445 μM MB, Aβ_{42} aggregated rapidly into oligomeric structures (Figure 3B). Immunoreactivity studies conducted under the same conditions (Figure 1A) show that these structures do not react with the A11 antibody even though they are morphologically similar to A11 positive oligomers (Figure 3C). These data suggest that these structures may represent A11-immunonegative fiber nuclei. After incubation for 5 days in the presence of MB, Aβ_{42} aggregated extensively into large structures that resemble fibril bundles (Figure 3D,F). The bundles contain well-defined fibers that are tightly aligned (Figure 5F, inset), and the size of the bundles appears to be on the scale of 100 nm to 1 μm. These data suggest that the high-molecular mass band detected at the top of the gel with 6E10 antibody in the presence of MB (Figure 2) consists of Aβ_{42} fibrils. In addition, these data suggest that the loss of 4G8 and 6E10 immunoreactivity observed on dot blots (Figure 1) at high concentrations of MB (445 μM) may be due both to the loss of antibody binding sites caused by Aβ_{42} aggregation and bundling and to weakened binding of Aβ_{42} fibrillar bundles to the membranes. Taken together, these data suggest that, under conditions described here, MB inhibits Aβ_{42} A11-immunoreactive oligomer formation, promotes fibrillization via promotion of formation of A11-immunonegative fiber nuclei, and promotes the formation of macroscopic fiber bundles.

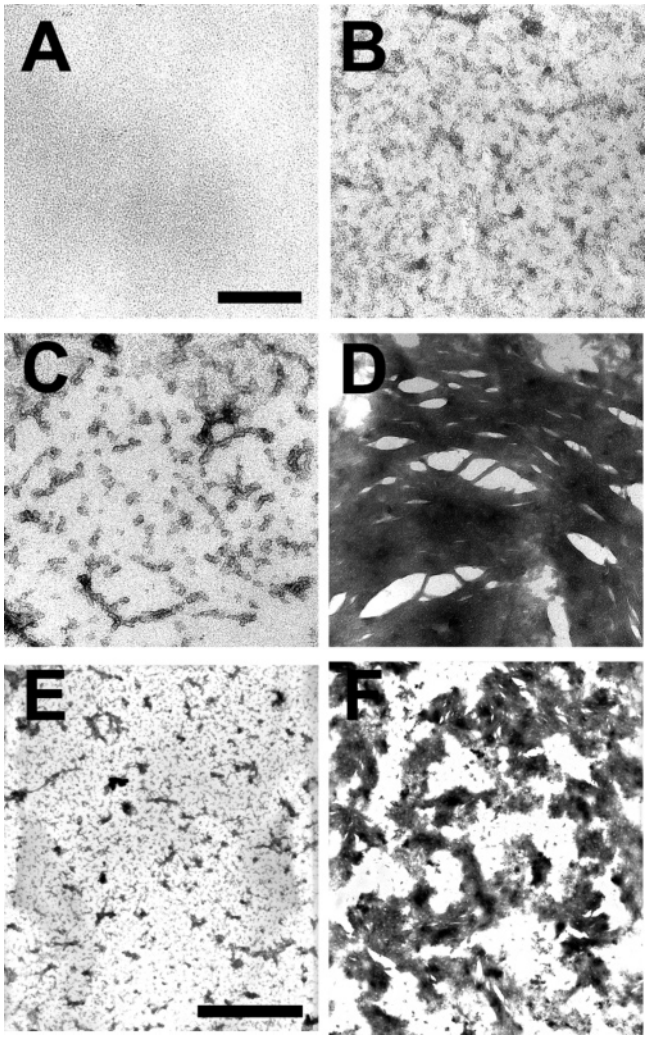

FIGURE 3: Fiber bundles accumulate in the presence of methylene blue. Aβ_{42} was incubated under oligomerization conditions without stirring (45 μM, final concentration) in the absence (A, C, and E) and presence (B, D, and F) of 445 μM MB. Aliquots of each reaction mixture were removed at various time points during aggregation and analyzed by TEM. In the control reaction, Aβ_{42} exhibited minimal aggregation at time zero (A) and formed a heterogeneous population of oligomers and protofibers within 5 days of the initiation of aggregation (C and E). In the presence of MB, Aβ_{42} exhibited signs of oligomerization at time zero (B) and aggregated into fibers that were heavily associated into bundles (D and F), 5 days after the initiation of aggregation. All images are cropped from TEM originals captured at 50000× magnification (bar = 150 nm) with the exception of data presented in panels E and F which represent images captured at 27000× magnification (bar = 1200 nm).

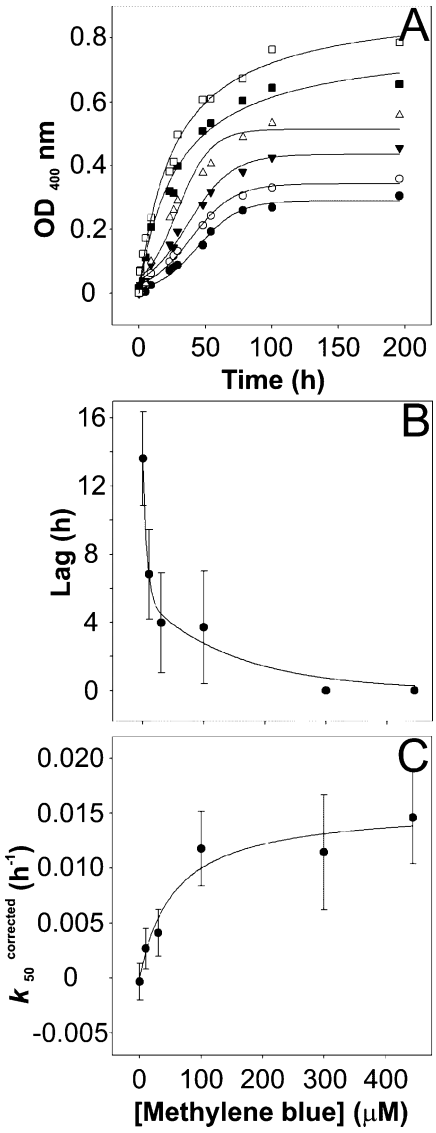

FIGURE 4: Methylene blue promotes Aβ_{42} fibrillization. Aβ_{42} was incubated under fibrillization conditions without stirring (45 μM, final concentration) for 8 days in the absence and presence of MB (10, 30, 100, 300, and 445 μM, final concentrations). (A) Aliquots of each reaction mixture were assayed at various time points by the turbidity captured at a wavelength of 400 nm. Under these conditions, Aβ_{42} (●) assembled into fibrils via nucleation-dependent kinetics. MB [10 (○), 30 (▼), 100 (△), 300 (■), and 445 μM (□)] promoted fibrillization in a dose-dependent manner. Each reading was corrected for the background absorbance corresponding to MB. Each curve represents the best fit of the data points to either eq 2 or 3. MB increased the amount of Aβ_{42} present in the aggregated form at equilibrium. (B) The lag time of assembly in the absence and presence of MB (10, 30, and 100 μM) was calculated from the sigmoidal assembly curves presented in panel A (eq 2). In the presence of higher concentrations of MB (300 and 445 μM), Aβ_{42} assembled without a lag time. In this case, the lag time was chosen to be zero, because these assembly reactions proceed in the absence of nucleation-dependent behavior. The decrease in the lag time observed in the presence of MB suggests that this compound promotes filament nucleation. (C) The fibrillization rates corresponding to half-maximal aggregation (k_{50}), or 50% fibrillization rates, were calculated in the absence and presence of MB from the assembly time courses presented in panel A (eqs 2 and 3). k_{50} obtained in the absence of MB was subtracted form all other rates and yielded $k_{50}^{\text{corrected}}$. Data points represent the $k_{50}^{\text{corrected}}$ value corresponding to each MB concentration. The curve represents a fit to eq 4 that yielded the MB concentration required to attain a half-maximal corrected 50% fibrillization rate. MB accelerates fibrillization in a dose-dependent manner.

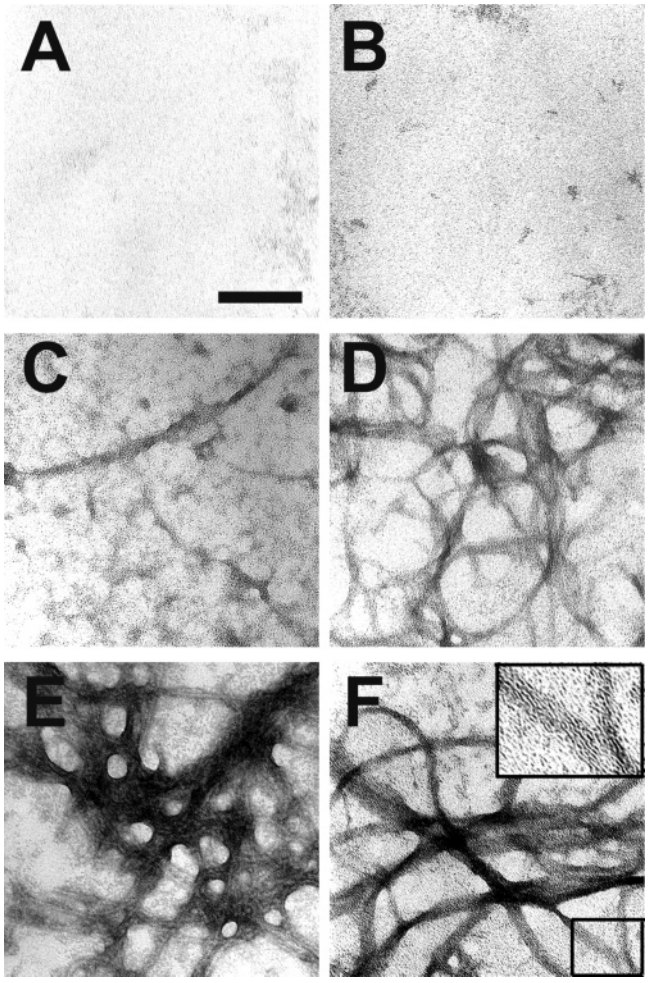

FIGURE 5: Methylene blue favors fiber bundle formation. Aliquots of the fibrillization reaction mixtures conducted in the absence (A, C, and E) or presence of 445 μM MB (B, D, and F) were imaged at various time points during aggregation. Aβ_{42} showed no signs of aggregation in the absence of MB and minimal aggregation in the presence of MB at time zero (A and B). Three days after the initiation of fibrillization, in the absence of MB, Aβ_{42} assembled into a heterogeneous population of protofibrils and fibrillar material (C). At the same time point during aggregation and in the presence of MB, Aβ_{42} formed well-defined, aligned, long fibers that tended to associate into curved bundles (D). Fibrillar structures continued to accumulate 5 days into the fibrillization reaction in the absence of MB (E). In contrast, in the presence of MB, Aβ_{42} aggregated into clumped, randomly oriented fiber bundles at this stage of aggregation (F). The inset is a high-magnification image of fiber bundle showing individual 6 nm fibers. All images are cropped from TEM originals captured at 50000× magnification (bar = 150 nm).

Methylene Blue Enhances Aβ_{42} Fibrillization. The data presented above suggest that in the presence of MB fiber formation is favored over oligomerization under conditions specially designed to support oligomer formation in control reactions (oligomerization conditions). Under these conditions, in the absence of MB, the aggregation reaction is slow and Aβ_{42} first forms fibril-free oligomers, making these conditions well-suited for oligomer studies. Eventually, Aβ_{42} assembles into fibers that coexist with oligomeric species (*37*). However, because the two species coexist at late time points (*37*), these conditions are not ideal for studies on homogeneous Aβ_{42} fibers. Therefore, for testing the effect of MB on Aβ_{42} fibrillization directly, Aβ_{42} was subjected to aggregation under conditions optimal for fibril formation

(fibrillization conditions), as described in Experimental Procedures. Under these conditions, Aβ_{42} assembles rapidly into fibrils (within 4 days) with classic 6−10 nm morphology, and the resulting fibrils are oligomer-free as determined by both A11 immunoreactivity and EM analysis (*37*). Aliquots of Aβ_{42} were removed at various time points in the absence (control reaction) or presence of MB (10, 30, 100, 300, and 445 μM) and assayed by turbidity at a wavelength of 400 nm. Parallel reactions lacking Aβ_{42} and containing MB were used to correct turbidity readings. This approach is appropriate because MB does not undergo spectral changes in the presence of various Aβ_{42} aggregated species used here. Consistent with previous observations (*37*), the time course of Aβ_{42} aggregation was nucleation-dependent, fit to a sigmoidal equation (eq 2), and reached plateau levels within 4 days (Figure 4A). The addition of MB, at concentrations up to 100 μM, did not change the nucleation-dependent behavior but increased equilibrium turbidity in a dose-dependent manner (Figure 4A). In contrast, in the presence of MB concentrations of >300 μM, Aβ_{42} fibrillization occurred without a lag time (Figure 4A) and the aggregation reactions fit well to rectangular hyperbolas (eq 3). The amount of aggregated Aβ_{42} obtained at equilibrium continued to increase in a dose-dependent manner. Overall, the amount of fibrillar Aβ_{42} observed at plateau levels increased exponentially as a function of MB concentration (fit not shown). The MB concentration required to attain half-maximal fibrillization was 173 ± 51.98 μM.

In the absence of MB, the lag time of Aβ_{42} fibrillization, calculated as described in Experimental Procedures, was 13.61 h (Figure 4B). Increasing concentrations of MB resulted in a dose-dependent decrease in lag time, to values that approached zero in the presence of ≥300 μM MB (Figure 4B). A dose-dependent increase in the fibrillization rate corresponding to half-maximal aggregation, $k_{50}^{\text{corrected}}$, which was calculated as described in Experimental Procedures (eq 4), was also observed (Figure 4C). The MB concentration required to attain a half-maximal corrected 50% fibrillization rate, calculated from a fit to a rectangular hyperbola, was 55.42 ± 22.77 μM (Figure 4C). Consistent with our prediction, the dose-dependent increase in the amount of aggregated Aβ_{42} observed in the presence of MB compared to control suggests that MB promotes fiber formation. In addition, the dose-dependent decrease in lag time and the increase in the 50% fibrillization rate suggest that MB promotes Aβ_{42} fibril formation by promoting fibril nucleation and enhancing the rate of fiber elongation.

To assess the morphology of the aggregated material obtained in the presence of MB under fibrillization conditions, aliquots of nontreated reaction mixtures and mixtures treated with 445 μM MB were removed at various time points and imaged by TEM. Consistent with previous observations (Figure 3A), in the absence of MB Aβ_{42} exhibited minimal aggregation at time zero (Figure 5A), started to aggregate into fibers with classical morphology after incubation for 3 days (Figure 5C), and fibrillized extensively upon prolonged incubation (5 days, Figure 5E). These fibers were predominantly straight individual fibers occasionally trapped into large clumps containing randomly oriented fibers (Figure 5E). Aβ_{42} aggregated rapidly in the presence of MB ($t = 0$, Figure 5B) and formed abundant fibrils associated into bundles (3 days, Figure 5D; 5 days, Figure 5F) longer than those observed under oligomerization conditions (Figure 3D,F). The addition of MB to preformed fibrils assembled under fibrillization conditions (similar to those in Figure 5E) changed their appearance to bundled fibers similar to those presented in Figure 5F, with no evidence of fiber loss (data not shown). Taken together, these data directly show that MB promotes Aβ_{42} fibrillization by enhancing filament nucleation and the rate of fiber elongation and promotes the bundling of individual fibrils. Enhancement of nucleation could be mediated by binding to nonoligomeric intermediates or small Aβ_{42} oligomers.

Methylene Blue Promotes the Fibrillization of Preformed Aβ_{42} Oligomers. To determine the effect of MB on preformed oligomers, Aβ_{42} was subjected to aggregation under oligomerization conditions for 4 days as described in Experimental Procedures. The oligomers were then split into equal volumes; one reaction mixture served as the control, and the others were supplied with MB (1−445 μM). Aliquots of each reaction mixture were analyzed by an ELISA using the anti-oligomer antibody A11, 2 days after the addition of MB. MB caused a dose-dependent, partial decrease in the amount of Aβ_{42} A11-immunoreactive oligomer. The IC_{50} for the inhibition of A11 immunoreactivity determined from the dose−response curve (eq 1) was 12.48 ± 3.28 μM (Figure 6A). These data suggest that MB induces a partial Aβ_{42} oligomer loss when added to preformed A11-immunoreactive oligomers at substoichiometric concentrations relative to that of the Aβ_{42} monomer.

To establish the nature of the species resulting from the treatment of preformed oligomers with MB, Aβ_{42} was subjected to oligomerization for 4 days under conditions described in Experimental Procedures. Immunoreactivity suggests that under these conditions Aβ_{42} forms oligomers reactive with anti-oligomer antibody A11 (Figures 1A and 6A and ref *37*). The oligomers were then split into three equal volumes; one reaction mixture served as the control, and the others were supplied with MB (10 and 445 μM) (time point zero of the oligomer disaggregation reaction). Aliquots of each reaction were removed at time points 0 and 7 days after treatment and imaged by TEM. In the absence of MB, and consistent with previous observations (*37*), Aβ_{42} oligomers used in this experiment appeared as heterogeneous sized particulate structures at time point zero (Figure 6B) and protofibrillar and fibrillar structures could be detected after prolonged incubation (7 days, Figure 6C). Low MB concentrations (10 μM) did not visibly alter aggregation (7 days, Figure 6D). Higher MB concentrations (445 μM) induced oligomer clumping and the formation of fibrils and fibril clumps (7 days, Figure 6E). The clumps formed in the presence of MB appear to consist of both oligomers and fibrils (Figure 6E). Taken together, these data suggest that, at substoichiometric concentrations relative to that of the Aβ_{42} monomer, MB promotes preformed oligomer clumping and fiber formation. This further suggests that MB may modulate Aβ_{42} aggregation, at least in part, via direct interaction with oligomers.

DISCUSSION

Recently, we identified a number of small molecules that specifically inhibit Aβ_{42} oligomerization without inhibiting fibril formation (*37*). MB is a novel class of oligomerization

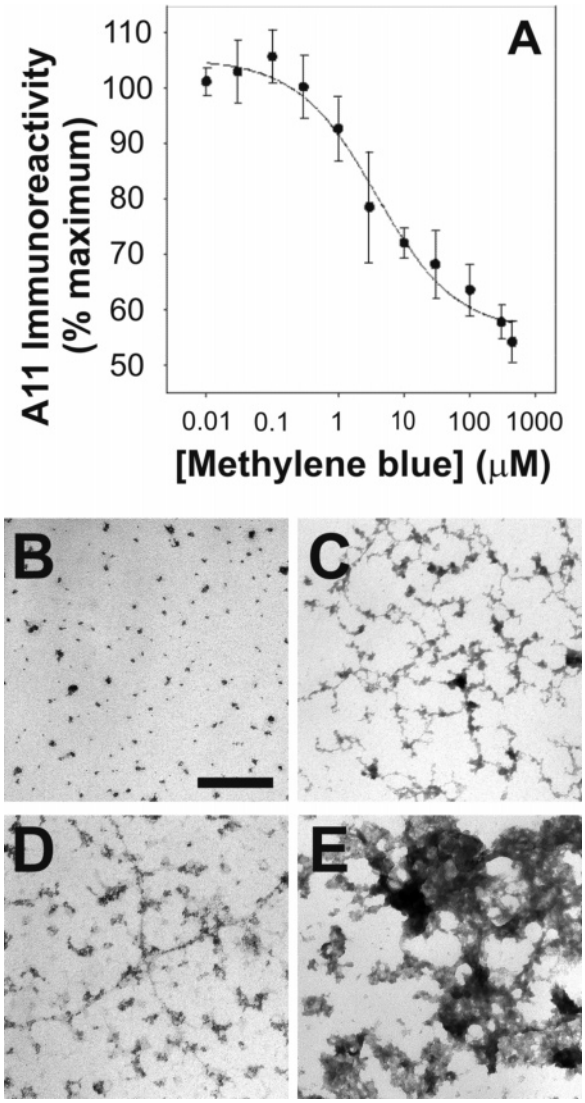

FIGURE 6: Methylene blue mediates partial preformed Aβ_{42} oligomer loss. Aβ_{42} was incubated under oligomerization conditions without stirring (45 μM, final concentration) for 4 days. The reaction mixture was then split into equal volumes; one served as a control, and others were supplemented with MB. (A) The ability of MB (0.01−445 μM) to induce oligomer loss was tested via an ELISA using anti-oligomer antibody A11, 2 days after MB was added to the preformed oligomers. Each data point was obtained in triplicate and is expressed as the percent absorbance of control reaction ± the standard deviation. The curve represents the best fit of the data points to eq 1 and yielded the IC_{50}. MB mediated partial oligomer loss. (B−E) Aβ_{42} oligomers were obtained under conditions described above (B) and then incubated without (C) or with MB (D and E) for an additional 7 days. In the absence of MB, Aβ_{42} preformed oligomers further associated into protofibers (C). Low concentrations of MB [10 μM (D)] did not dramatically interfere with the progression of the aggregation reaction. In contrast, 445 μM MB promoted preformed oligomer clumping and progression to fibrillar structure (E). All samples were imaged by TEM at 22000× magnification, and the resulting images were processed in Adobe Photoshop (bar = 150 nm).

inhibitors that acts by promoting fibril formation. Besides the fact that they are pharmacologically interesting, this observation suggests that oligomer and fibril formation are competing pathways of Aβ aggregation. MB has many properties desired from drug candidates expected to act in the brain (*60*−*62*) and is approved for use in humans (*61*, *63*). These characteristics, together with initial evidence that MB could bind disease lesions (*80*−*86*) and interfere with protein aggregation (*66*, *71*), suggest that MB could be used as a therapeutic agent and a tool in understanding the pathological significance of amyloid oligomers and fibrils in transgenic animal models of AD.

We used two different reaction conditions to test the ability of MB to modulate Aβ_{42} assembly. One of the conditions favors Aβ_{42} oligomerization and enables the examination of fiber-free oligomers at early stages of aggregation (*37*). The second condition favors Aβ_{42} fibrillization and yields oligomer-free fibers (*37*). Detection of oligomer formation relies primarily on immunoreactivity with the anti-oligomer-specific antibody, A11 (*1*), while fiber formation is assayed by turbidity (*18*, *78*). To confirm the results of both assays, the nature of the aggregated material is analyzed by TEM. Unlike other small molecules (*73*, *87*), MB does not undergo spectral changes in the presence of any of the Aβ_{42} species used in this study (data not shown). Therefore, turbidity is a reliable method for assaying fiber formation in this case and avoids potential artifacts that could be encountered in screens based on ThT fluorescence conducted in the presence of small molecules (*73*, *88*, *89*). By taking advantage of the means described above, we separately screened the ability of MB to modulate Aβ_{42} oligomer and fiber formation.

It has been long known that Aβ_{42} assembles through nucleation-dependent kinetics (*3*, *4*). The pathway leading to fibrillization starts when misfolded or unfolded proteins aggregate or adopt a conformation that leads to the formation of a nucleus that is capable of elongating by recruiting additional misfolded subunits. Since the formation of the nucleus is rate-limiting, the appearance of nuclei represents a commitment toward fibrillization. The end result of this process is the formation of amyloid fibers. Recent evidence suggests that Aβ_{42} assembly is a more complex phenomenon, and the description above represents only one branch of the pathway. The assembly pathway is also populated with numerous other species, including pre-nucleation assembly intermediates, oligomers, protofibrils, annular protofibrils, and polymorphic fibrillar structures (*1*, *27*, *39*, *40*, *42*, *44*, *47*, *50*, *51*, *90*−*92*). The relationship among these species is poorly understood, and their presence on the same aggregation pathway is uncertain. Under the fibrillization conditions used here, Aβ_{42} forms fibers in a classic nucleation-dependent manner, in the absence of oligomeric intermediates (fibrillization pathway) (*37*). In contrast, oligomerization conditions favor oligomer formation at early time points through a different pathway (oligomerization pathway), although fibers ultimately form under these oligomerization conditions (*37*).

MB influences both the oligomerization and fibrillization pathways. MB inhibits oligomerization at substoichiometric concentrations relative to that of the Aβ_{42} monomer. However, MB does not prevent Aβ_{42} aggregation but rather appears to favor association into aggregates that nucleate fibril formation. The observation that increasing concentrations of MB decrease the assembly lag time, a parameter that reflects fibril nucleation (*79*), is consistent with the promotion of Aβ_{42} nucleation by MB. Indeed, high concentrations of MB completely abolish the nucleation-dependent behavior of Aβ_{42} fibrillization and simulate assembly kinetics obtained in the presence of seeding. This suggests that MB could stabilize prenuclear Aβ_{42} assembly competent intermediates, favoring nucleation and driving the protein into the nucleation-dependent assembly pathway (fibrillization

pathway). The inhibition of Aβ_{42} oligomerization concomitant with the promotion of fiber formation could occur solely by depleting the monomer pool required for oligomerization. Stabilization of assembly competent intermediates was also reported to mediate the assembly of tau, α-synuclein, and amylin (*74*, *76*, *77*, *79*, *93*−*95*). The fact that MB promotes fibril formation upon addition to preformed oligomers suggests that this conformational templating is not limited to Aβ monomers and may include small oligomers.

In addition, MB may promote filament elongation, consistent with its ability to increase the 50% fibrillization rate in a concentration-dependent manner. MB-stabilized assembly competent intermediates and MB-bound small oligomers could adhere more easily to preformed nuclei and fibers and facilitate filament elongation. At high concentrations, MB supports fibril association and formation of fibrillar bundles that could be useful for structural characterization. Taken together, these data show that MB inhibits Aβ_{42} oligomerization by promoting fibrillization. Whether this phenomenon occurs entirely via the trapping of the majority of Aβ_{42} in the nucleation-dependent assembly pathway or occurs in part through the oligomer-dependent assembly pathway remains to be elucidated. Since the Aβ_{42} fibrillar species are less toxic than oligomers and may even be protective, modulating aggregation through this mechanism could be pharmacologically attractive.

REFERENCES

1. Kayed, R., Head, E., Thompson, J. L., McIntire, T. M., Milton, S. C., Cotman, C. W., and Glabe, C. G. (2003) Common structure of soluble amyloid oligomers implies common mechanism of pathogenesis, *Science 300*, 486−489.
2. Selkoe, D. J. (1991) The molecular pathology of Alzheimer's disease, *Neuron 6*, 487−498.
3. Jarrett, J. T., Berger, E. P., and Lansbury, P. T., Jr. (1993) The carboxy terminus of the β amyloid protein is critical for the seeding of amyloid formation: Implications for the pathogenesis of Alzheimer's disease, *Biochemistry 32*, 4693−4697.
4. Harper, J. D., and Lansbury, P. T., Jr. (1997) Models of amyloid seeding in Alzheimer's disease and scrapie: Mechanistic truths and physiological consequences of the time-dependent solubility of amyloid proteins, *Annu. Rev. Biochem. 66*, 385−407.
5. Howlett, D. R., Jennings, K. H., Lee, D. C., Clark, M. S., Brown, F., Wetzel, R., Wood, S. J., Camilleri, P., and Roberts, G. W. (1995) Aggregation state and neurotoxic properties of Alzheimer β-amyloid peptide, *Neurodegeneration 4*, 23−32.
6. Pike, C. J., Walencewicz, A. J., Glabe, C. G., and Cotman, C. W. (1991) In vitro aging of β-amyloid protein causes peptide aggregation and neurotoxicity, *Brain Res. 563*, 311−314.
7. Pike, C. J., Burdick, D., Walencewicz, A. J., Glabe, C. G., and Cotman, C. W. (1993) Neurodegeneration induced by β-amyloid peptides in vitro: The role of peptide assembly state, *J. Neurosci. 13*, 1676−1687.
8. Seilheimer, B., Bohrmann, B., Bondolfi, L., Muller, F., Stuber, D., and Dobeli, H. (1997) The toxicity of the Alzheimer's β-amyloid peptide correlates with a distinct fiber morphology, *J. Struct. Biol. 119*, 59−71.
9. Lorenzo, A., and Yankner, B. A. (1994) β-Amyloid neurotoxicity requires fibril formation and is inhibited by congo red, *Proc. Natl. Acad. Sci. U.S.A. 91*, 12243−12247.
10. Sabate, R., and Estelrich, J. (2005) Stimulatory and inhibitory effects of alkyl bromide surfactants on β-amyloid fibrillogenesis, *Langmuir 21*, 6944−6949.
11. Kuner, P., Bohrmann, B., Tjernberg, L. O., Naslund, J., Huber, G., Celenk, S., Gruninger-Leitch, F., Richards, J. G., Jakob-Roetne, R., Kemp, J. A., and Nordstedt, C. (2000) Controlling polymerization of β-amyloid and prion-derived peptides with synthetic small molecule ligands, *J. Biol. Chem. 275*, 1673−1678.
12. Ono, K., Hasegawa, K., Naiki, H., and Yamada, M. (2004) Curcumin has potent anti-amyloidogenic effects for Alzheimer's β-amyloid fibrils in vitro, *J. Neurosci. Res. 75*, 742−750.
13. Cheng, X., and van Breemen, R. B. (2005) Mass spectrometry-based screening for inhibitors of β-amyloid protein aggregation, *Anal. Chem. 77*, 7012−7015.
14. De Felice, F. G., Houzel, J. C., Garcia-Abreu, J., Louzada, P. R., Jr., Afonso, R. C., Meirelles, M. N., Lent, R., Neto, V. M., and Ferreira, S. T. (2001) Inhibition of Alzheimer's disease β-amyloid aggregation, neurotoxicity, and in vivo deposition by nitrophenols: Implications for Alzheimer's therapy, *FASEB J. 15*, 1297−1299.
15. Bohrmann, B., Adrian, M., Dubochet, J., Kuner, P., Muller, F., Huber, W., Nordstedt, C., and Dobeli, H. (2000) Self-assembly of β-amyloid 42 is retarded by small molecular ligands at the stage of structural intermediates, *J. Struct. Biol. 130*, 232−246.
16. Howlett, D. R., George, A. R., Owen, D. E., Ward, R. V., and Markwell, R. E. (1999) Common structural features determine the effectiveness of carvedilol, daunomycin and rolitetracycline as inhibitors of Alzheimer β-amyloid fibril formation, *Biochem. J. 343* (Part 2), 419−423.
17. Tomiyama, T., Asano, S., Suwa, Y., Morita, T., Kataoka, K., Mori, H., and Endo, N. (1994) Rifampicin prevents the aggregation and neurotoxicity of amyloid β protein in vitro, *Biochem. Biophys. Res. Commun. 204*, 76−83.
18. Wood, S. J., MacKenzie, L., Maleeff, B., Hurle, M. R., and Wetzel, R. (1996) Selective inhibition of Aβ fibril formation, *J. Biol. Chem. 271*, 4086−4092.
19. Pappolla, M., Bozner, P., Soto, C., Shao, H., Robakis, N. K., Zagorski, M., Frangione, B., and Ghiso, J. (1998) Inhibition of Alzheimer β-fibrillogenesis by melatonin, *J. Biol. Chem. 273*, 7185−7188.
20. Lashuel, H. A., Hartley, D. M., Balakhaneh, D., Aggarwal, A., Teichberg, S., and Callaway, D. J. (2002) New class of inhibitors of amyloid-β fibril formation. Implications for the mechanism of pathogenesis in Alzheimer's disease, *J. Biol. Chem. 277*, 42881−42890.
21. Howlett, D. R., Perry, A. E., Godfrey, F., Swatton, J. E., Jennings, K. H., Spitzfaden, C., Wadsworth, H., Wood, S. J., and Markwell, R. E. (1999) Inhibition of fibril formation in β-amyloid peptide by a novel series of benzofurans, *Biochem. J. 340* (Part 1), 283−289.
22. Williams, A. D., Sega, M., Chen, M., Kheterpal, I., Geva, M., Berthelier, V., Kaleta, D. T., Cook, K. D., and Wetzel, R. (2005) Structural properties of Aβ protofibrils stabilized by a small molecule, *Proc. Natl. Acad. Sci. U.S.A. 102*, 7115−7120.
23. Ono, K., Hasegawa, K., Naiki, H., and Yamada, M. (2004) Anti-amyloidogenic activity of tannic acid and its activity to destabilize Alzheimer's β-amyloid fibrils in vitro, *Biochim. Biophys. Acta 1690*, 193−202.
24. De Felice, F. G., Vieira, M. N., Saraiva, L. M., Figueroa-Villar, J. D., Garcia-Abreu, J., Liu, R., Chang, L., Klein, W. L., and Ferreira, S. T. (2004) Targeting the neurotoxic species in Alzheimer's disease: Inhibitors of Aβ oligomerization, *FASEB J. 18*, 1366−1372.
25. Pollack, S. J., Sadler, I. I., Hawtin, S. R., Tailor, V. J., and Shearman, M. S. (1995) Sulfonated dyes attenuate the toxic effects of β-amyloid in a structure-specific fashion, *Neurosci. Lett. 197*, 211−214.
26. Terry, R. D., Masliah, E., Salmon, D. P., Butters, N., DeTeresa, R., Hill, R., Hansen, L. A., and Katzman, R. (1991) Physical basis of cognitive alterations in Alzheimer's disease: Synapse loss is the major correlate of cognitive impairment, *Ann. Neurol. 30*, 572−580.
27. Lambert, M. P., Barlow, A. K., Chromy, B. A., Edwards, C., Freed, R., Liosatos, M., Morgan, T. E., Rozovsky, I., Trommer, B., Viola, K. L., Wals, P., Zhang, C., Finch, C. E., Krafft, G. A., and Klein, W. L. (1998) Diffusible, nonfibrillar ligands derived from Aβ1−42 are potent central nervous system neurotoxins, *Proc. Natl. Acad. Sci. U.S.A. 95*, 6448−6453.
28. Hartley, D. M., Walsh, D. M., Ye, C. P., Diehl, T., Vasquez, S., Vassilev, P. M., Teplow, D. B., and Selkoe, D. J. (1999) Protofibrillar intermediates of amyloid β-protein induce acute electrophysiological changes and progressive neurotoxicity in cortical neurons, *J. Neurosci. 19*, 8876−8884.
29. Walsh, D. M., Klyubin, I., Fadeeva, J. V., Cullen, W. K., Anwyl, R., Wolfe, M. S., Rowan, M. J., and Selkoe, D. J. (2002) Naturally secreted oligomers of amyloid β protein potently inhibit hippocampal long-term potentiation in vivo, *Nature 416*, 535−539.

30. Dahlgren, K. N., Manelli, A. M., Stine, W. B., Jr., Baker, L. K., Krafft, G. A., and LaDu, M. J. (2002) Oligomeric and fibrillar species of amyloid-β peptides differentially affect neuronal viability, *J. Biol. Chem. 277*, 32046−32053.
31. Hoshi, M., Sato, M., Matsumoto, S., Noguchi, A., Yasutake, K., Yoshida, N., and Sato, K. (2003) Spherical aggregates of β-amyloid (amylospheroid) show high neurotoxicity and activate tau protein kinase I/glycogen synthase kinase-3β, *Proc. Natl. Acad. Sci. U.S.A. 100*, 6370−6375.
32. Klein, W. L., Krafft, G. A., and Finch, C. E. (2001) Targeting small Aβ oligomers: The solution to an Alzheimer's disease conundrum? *Trends Neurosci. 24*, 219−224.
33. Caughey, B., and Lansbury, P. T. (2003) Protofibrils, pores, fibrils, and neurodegeneration: Separating the responsible protein aggregates from the innocent bystanders, *Annu. Rev. Neurosci. 26*, 267−298.
34. Klein, W. L., Stine, W. B., Jr., and Teplow, D. B. (2004) Small assemblies of unmodified amyloid β-protein are the proximate neurotoxin in Alzheimer's disease, *Neurobiol. Aging 25*, 569−580.
35. McLean, C. A., Cherny, R. A., Fraser, F. W., Fuller, S. J., Smith, M. J., Beyreuther, K., Bush, A. I., and Masters, C. L. (1999) Soluble pool of Aβ amyloid as a determinant of severity of neurodegeneration in Alzheimer's disease, *Ann. Neurol. 46*, 860−866.
36. Lue, L. F., Kuo, Y. M., Roher, A. E., Brachova, L., Shen, Y., Sue, L., Beach, T., Kurth, J. H., Rydel, R. E., and Rogers, J. (1999) Soluble amyloid β peptide concentration as a predictor of synaptic change in Alzheimer's disease, *Am. J. Pathol. 155*, 853−862.
37. Necula, M., Kayed, R., Milton, S., and Glabe, C. G. (2007) Small-molecule inhibitors distinguish between amyloid β oligomerization and fibrillization pathways, *J. Biol. Chem. 282*, 10311−10324.
38. Gorman, P. M., Yip, C. M., Fraser, P. E., and Chakrabartty, A. (2003) Alternate aggregation pathways of the Alzheimer β-amyloid peptide: Aβ association kinetics at endosomal pH, *J. Mol. Biol. 325*, 743−757.
39. Soreghan, B., Kosmoski, J., and Glabe, C. (1994) Surfactant properties of Alzheimer's A β peptides and the mechanism of amyloid aggregation, *J. Biol. Chem. 269*, 28551−28554.
40. Harper, J. D., Lieber, C. M., and Lansbury, P. T., Jr. (1997) Atomic force microscopic imaging of seeded fibril formation and fibril branching by the Alzheimer's disease amyloid-β protein, *Chem. Biol. 4*, 951−959.
41. Yong, W., Lomakin, A., Kirkitadze, M. D., Teplow, D. B., Chen, S. H., and Benedek, G. B. (2002) Structure determination of micelle-like intermediates in amyloid β-protein fibril assembly by using small angle neutron scattering, *Proc. Natl. Acad. Sci. U.S.A. 99*, 150−154.
42. Lomakin, A., Teplow, D. B., Kirschner, D. A., and Benedek, G. B. (1997) Kinetic theory of fibrillogenesis of amyloid β-protein, *Proc. Natl. Acad. Sci. U.S.A. 94*, 7942−7947.
43. Huang, T. H., Yang, D. S., Plaskos, N. P., Go, S., Yip, C. M., Fraser, P. E., and Chakrabartty, A. (2000) Structural studies of soluble oligomers of the Alzheimer β-amyloid peptide, *J. Mol. Biol. 297*, 73−87.
44. Kuo, Y. M., Emmerling, M. R., Vigo-Pelfrey, C., Kasunic, T. C., Kirkpatrick, J. B., Murdoch, G. H., Ball, M. J., and Roher, A. E. (1996) Water-soluble Aβ (N-40, N-42) oligomers in normal and Alzheimer disease brains, *J. Biol. Chem. 271*, 4077−4081.
45. Roher, A. E., Chaney, M. O., Kuo, Y. M., Webster, S. D., Stine, W. B., Haverkamp, L. J., Woods, A. S., Cotter, R. J., Tuohy, J. M., Krafft, G. A., Bonnell, B. S., and Emmerling, M. R. (1996) Morphology and toxicity of Aβ-(1−42) dimer derived from neuritic and vascular amyloid deposits of Alzheimer's disease, *J. Biol. Chem. 271*, 20631−20635.
46. Walsh, D. M., Lomakin, A., Benedek, G. B., Condron, M. M., and Teplow, D. B. (1997) Amyloid β-protein fibrillogenesis. Detection of a protofibrillar intermediate, *J. Biol. Chem. 272*, 22364−22372.
47. Harper, J. D., Wong, S. S., Lieber, C. M., and Lansbury, P. T. (1997) Observation of metastable Aβ amyloid protofibrils by atomic force microscopy, *Chem. Biol. 4*, 119−125.
48. Blackley, H. K., Sanders, G. H., Davies, M. C., Roberts, C. J., Tendler, S. J., and Wilkinson, M. J. (2000) In-situ atomic force microscopy study of β-amyloid fibrillization, *J. Mol. Biol. 298*, 833−840.
49. Nybo, M., Svehag, S. E., and Holm Nielsen, E. (1999) An ultrastructural study of amyloid intermediates in Aβ1−42 fibrillogenesis, *Scand. J. Immunol. 49*, 219−223.
50. Walsh, D. M., Hartley, D. M., Kusumoto, Y., Fezoui, Y., Condron, M. M., Lomakin, A., Benedek, G. B., Selkoe, D. J., and Teplow, D. B. (1999) Amyloid β-protein fibrillogenesis. Structure and biological activity of protofibrillar intermediates, *J. Biol. Chem. 274*, 25945−25952.
51. Kirkitadze, M. D., Condron, M. M., and Teplow, D. B. (2001) Identification and characterization of key kinetic intermediates in amyloid β-protein fibrillogenesis, *J. Mol. Biol. 312*, 1103−1119.
52. Naiki, H., and Nakakuki, K. (1996) First-order kinetic model of Alzheimer's β-amyloid fibril extension in vitro, *Lab. Invest. 74*, 374−383.
53. Lomakin, A., Chung, D. S., Benedek, G. B., Kirschner, D. A., and Teplow, D. B. (1996) On the nucleation and growth of amyloid β-protein fibrils: Detection of nuclei and quantitation of rate constants, *Proc. Natl. Acad. Sci. U.S.A. 93*, 1125−1129.
54. Harper, J. D., Wong, S. S., Lieber, C. M., and Lansbury, P. T., Jr. (1999) Assembly of Aβ amyloid protofibrils: An in vitro model for a possible early event in Alzheimer's disease, *Biochemistry 38*, 8972−8980.
55. Chromy, B. A., Nowak, R. J., Lambert, M. P., Viola, K. L., Chang, L., Velasco, P. T., Jones, B. W., Fernandez, S. J., Lacor, P. N., Horowitz, P., Finch, C. E., Krafft, G. A., and Klein, W. L. (2003) Self-assembly of Aβ(1−42) into globular neurotoxins, *Biochemistry 42*, 12749−12760.
56. Yao, Z., Drieu, K., and Papadopoulos, V. (2001) The Ginkgo biloba extract EGb 761 rescues the PC12 neuronal cells from β-amyloid-induced cell death by inhibiting the formation of β-amyloid-derived diffusible neurotoxic ligands, *Brain Res. 889*, 181−190.
57. Podlisny, M. B., Walsh, D. M., Amarante, P., Ostaszewski, B. L., Stimson, E. R., Maggio, J. E., Teplow, D. B., and Selkoe, D. J. (1998) Oligomerization of endogenous and synthetic amyloid β-protein at nanomolar levels in cell culture and stabilization of monomer by Congo red, *Biochemistry 37*, 3602−3611.
58. Chang, L., Bakhos, L., Wang, Z., Venton, D. L., and Klein, W. L. (2003) Femtomole immunodetection of synthetic and endogenous amyloid-β oligomers and its application to Alzheimer's disease drug candidate screening, *J. Mol. Neurosci. 20*, 305−313.
59. Yang, F., Lim, G. P., Begum, A. N., Ubeda, O. J., Simmons, M. R., Ambegaokar, S. S., Chen, P. P., Kayed, R., Glabe, C. G., Frautschy, S. A., and Cole, G. M. (2005) Curcumin inhibits formation of amyloid β oligomers and fibrils, binds plaques, and reduces amyloid in vivo, *J. Biol. Chem. 280*, 5892−5901.
60. Riha, P. D., Bruchey, A. K., Echevarria, D. J., and Gonzalez-Lima, F. (2005) Memory facilitation by methylene blue: Dose-dependent effect on behavior and brain oxygen consumption, *Eur. J. Pharmacol. 511*, 151−158.
61. Kupfer, A., Aeschlimann, C., Wermuth, B., and Cerny, T. (1994) Prophylaxis and reversal of ifosfamide encephalopathy with methylene-blue, *Lancet 343*, 763−764.
62. Peter, C., Hongwan, D., Kupfer, A., and Lauterburg, B. H. (2000) Pharmacokinetics and organ distribution of intravenous and oral methylene blue, *Eur. J. Clin. Pharmacol. 56*, 247−250.
63. DiSanto, A. R., and Wagner, J. G. (1972) Pharmacokinetics of highly ionized drugs. II. Methylene blue: Absorption, metabolism, and excretion in man and dog after oral administration, *J. Pharm. Sci. 61*, 1086−1090.
64. Riedel, W., Lang, U., Oetjen, U., Schlapp, U., and Shibata, M. (2003) Inhibition of oxygen radical formation by methylene blue, aspirin, or α-lipoic acid, prevents bacterial-lipopolysaccharide-induced fever, *Mol. Cell. Biochem. 247*, 83−94.
65. Callaway, N. L., Riha, P. D., Wrubel, K. M., McCollum, D., and Gonzalez-Lima, F. (2002) Methylene blue restores spatial memory retention impaired by an inhibitor of cytochrome oxidase in rats, *Neurosci. Lett. 332*, 83−86.
66. Taniguchi, S., Suzuki, N., Masuda, M., Hisanaga, S., Iwatsubo, T., Goedert, M., and Hasegawa, M. (2005) Inhibition of heparin-induced tau filament formation by phenothiazines, polyphenols, and porphyrins, *J. Biol. Chem. 280*, 7614−7623.
67. Roikhel, V. M., Fokina, G. I., and Pogodina, V. V. (1984) Influence of aminasine on experimental scrapie in mice, *Acta Virol. 28*, 321−324.
68. Dees, C., Wade, W. F., German, T. L., and Marsh, R. F. (1985) Inactivation of the scrapie agent by ultraviolet irradiation in the presence of chlorpromazine, *J. Gen. Virol. 66* (Part 4), 845−849.
69. Doh-Ura, K., Iwaki, T., and Caughey, B. (2000) Lysosomotropic agents and cysteine protease inhibitors inhibit scrapie-associated prion protein accumulation, *J. Virol. 74*, 4894−4897.

70. Korth, C., May, B. C., Cohen, F. E., and Prusiner, S. B. (2001) Acridine and phenothiazine derivatives as pharmacotherapeutics for prion disease, *Proc. Natl. Acad. Sci. U.S.A. 98*, 9836−9841.
71. Wischik, C. M., Edwards, P. C., Lai, R. Y., Roth, M., and Harrington, C. R. (1996) Selective inhibition of Alzheimer disease-like tau aggregation by phenothiazines, *Proc. Natl. Acad. Sci. U.S.A. 93*, 11213−11218.
72. Burdick, D., Soreghan, B., Kwon, M., Kosmoski, J., Knauer, M., Henschen, A., Yates, J., Cotman, C., and Glabe, C. (1992) Assembly and aggregation properties of synthetic Alzheimer's A4/β amyloid peptide analogs, *J. Biol. Chem. 267*, 546−554.
73. Necula, M., Chirita, C. N., and Kuret, J. (2005) Cyanine dye N744 inhibits tau fibrillization by blocking filament extension: Implications for the treatment of tauopathic neurodegenerative diseases, *Biochemistry 44*, 10227−10237.
74. Uversky, V. N., Li, J., and Fink, A. L. (2001) Evidence for a partially folded intermediate in α-synuclein fibril formation, *J. Biol. Chem. 276*, 10737−10744.
75. Nielsen, L., Khurana, R., Coats, A., Frokjaer, S., Brange, J., Vyas, S., Uversky, V. N., and Fink, A. L. (2001) Effect of environmental factors on the kinetics of insulin fibril formation: Elucidation of the molecular mechanism, *Biochemistry 40*, 6036−6046.
76. Chirita, C. N., and Kuret, J. (2004) Evidence for an intermediate in tau filament formation, *Biochemistry 43*, 1704−1714.
77. Necula, M., Chirita, C. N., and Kuret, J. (2003) Rapid anionic micelle-mediated α-synuclein fibrillization in vitro, *J. Biol. Chem. 278*, 46674−46680.
78. Evans, K. C., Berger, E. P., Cho, C. G., Weisgraber, K. H., and Lansbury, P. T., Jr. (1995) Apolipoprotein E is a kinetic but not a thermodynamic inhibitor of amyloid formation: Implications for the pathogenesis and treatment of Alzheimer disease, *Proc. Natl. Acad. Sci. U.S.A. 92*, 763−767.
79. Chirita, C. N., Necula, M., and Kuret, J. (2003) Anionic micelles and vesicles induce tau fibrillization in vitro, *J. Biol. Chem. 278*, 25644−25650.
80. Jiao, Q., and Liu, Q. (1999) Characterization of the interaction between methylene blue and glycosaminoglycans, *Spectrochim. Acta, Part A 55*, 1667−1673.
81. Snow, A. D., Lara, S., Nochlin, D., and Wight, T. N. (1989) Cationic dyes reveal proteoglycans structurally integrated within the characteristic lesions of Alzheimer's disease, *Acta Neuropathol. 78*, 113−123.
82. Snow, A. D., Mar, H., Nochlin, D., Kimata, K., Kato, M., Suzuki, S., Hassell, J., and Wight, T. N. (1988) The presence of heparan sulfate proteoglycans in the neuritic plaques and congophilic angiopathy in Alzheimer's disease, *Am. J. Pathol. 133*, 456−463.
83. Su, J. H., Cummings, B. J., and Cotman, C. W. (1992) Localization of heparan sulfate glycosaminoglycan and proteoglycan core protein in aged brain and Alzheimer's disease, *Neuroscience 51*, 801−813.
84. Snow, A. D., Mar, H., Nochlin, D., Kresse, H., and Wight, T. N. (1992) Peripheral distribution of dermatan sulfate proteoglycans (decorin) in amyloid-containing plaques and their presence in neurofibrillary tangles of Alzheimer's disease, *J. Histochem. Cytochem. 40*, 105−113.
85. Snow, A. D., Nochlin, D., Sekiguichi, R., and Carlson, S. S. (1996) Identification in immunolocalization of a new class of proteoglycan (keratan sulfate) to the neuritic plaques of Alzheimer's disease, *Exp. Neurol. 138*, 305−317.
86. DeWitt, D. A., Silver, J., Canning, D. R., and Perry, G. (1993) Chondroitin sulfate proteoglycans are associated with the lesions of Alzheimer's disease, *Exp. Neurol. 121*, 149−152.
87. Nilsson, K. P., Herland, A., Hammarstrom, P., and Inganas, O. (2005) Conjugated polyelectrolytes: Conformation-sensitive optical probes for detection of amyloid fibril formation, *Biochemistry 44*, 3718−3724.
88. Kim, Y. S., Randolph, T. W., Manning, M. C., Stevens, F. J., and Carpenter, J. F. (2003) Congo red populates partially unfolded states of an amyloidogenic protein to enhance aggregation and amyloid fibril formation, *J. Biol. Chem. 278*, 10842−10850.
89. Souillac, P. O., Uversky, V. N., Millett, I. S., Khurana, R., Doniach, S., and Fink, A. L. (2002) Elucidation of the molecular mechanism during the early events in immunoglobulin light chain amyloid fibrillation. Evidence for an off-pathway oligomer at acidic pH, *J. Biol. Chem. 277*, 12666−12679.
90. Serpell, L. C. (2000) Alzheimer's amyloid fibrils: Structure and assembly, *Biochim. Biophys. Acta 1502*, 16−30.
91. Santini, S., Wei, G., Mousseau, N., and Derreumaux, P. (2004) Pathway complexity of Alzheimer's β-amyloid Aβ16−22 peptide assembly, *Structure 12*, 1245−1255.
92. Lashuel, H. A., Hartley, D. M., Petre, B. M., Wall, J. S., Simon, M. N., Walz, T., and Lansbury, P. T., Jr. (2003) Mixtures of wild-type and a pathogenic (E22G) form of Aβ40 in vitro accumulate protofibrils, including amyloid pores, *J. Mol. Biol. 332*, 795−808.
93. Kayed, R., Bernhagen, J., Greenfield, N., Sweimeh, K., Brunner, H., Voelter, W., and Kapurniotu, A. (1999) Conformational transitions of islet amyloid polypeptide (IAPP) in amyloid formation in vitro, *J. Mol. Biol. 287*, 781−796.
94. Uversky, V. N., Lee, H. J., Li, J., Fink, A. L., and Lee, S. J. (2001) Stabilization of partially folded conformation during α-synuclein oligomerization in both purified and cytosolic preparations, *J. Biol. Chem. 276*, 43495−43498.
95. Chirita, C. N., Congdon, E. E., Yin, H., and Kuret, J. (2005) Triggers of full-length tau aggregation: A role for partially folded intermediates, *Biochemistry 44*, 5862−5872.

BI700411K